Design Report

1. Introduction

Finding the optimal bridge dimensions required several considerations, the key ones being the factor of safety (FOS) of compression and the factor of safety of shear buckling, as in every scenario we generated they were the lowest, indicating high likelihood of failure. In order to increase the factor of safety, the thickness of the surface (which we often refer to as the "top sheet") and the ȳ value were both increased. Increasing the thickness of the top sheet was essential, as the maximum stress that it is able to endure at that point is proportional to thickness (t), following the $\frac{K\pi^2 E}{12(1-\mu^2)}(\frac{t}{b})^2$ equation. ȳ was raised in order to decrease the maximum stress experienced at the top, increasing factor of safety of compression. These adjustments were kept in mind when iterating, alongside that fact that our design must be realistic (i.e, fit the matboard dimensions).

1.1 Final Design - Design # 5

Our final product involved a beam composed of different sections of varied lengths. While simulating load with the computer program we created, we noticed that different components of the bridge experienced different stress than others. This enables us to be more efficient (in saving material) in certain sections, especially the middle, where we decided to remove the base of the bridge. In addition, removing the base of the middle section raised our ȳ, as required. However, in this middle 210 mm section, where flexural compression is the strongest, we decided to triple layer the top sheet so the "y-top" distance was decreased, thus the stress applied is also decreased. Additionally, the middle section has a deck width of 100 mm and height of 130 mm. The remaining areas of the bridge all had a base with dimensions of a 120 mm deck width, with only two layers on the top sheet and a height of 120 mm. The base widths of all sections are 60 mm, with 130 mm diaphragm spacings. Overall, this design was our most efficient and functional with a calculated factor of safety of 3.22 (Due to . However, when testing, we believe that this factor of safety will be lowered to around 2 (800N) due design calculations such as the splicing FOS, that cannot be calculated given the limitations of this project.

2. Iterations

2.1 Design 0

After performing the required calculations for design zero, we found promising results that proved this design to be a good starting point to begin iterating. However, certain factors of safety results were concerning, one being the factor of safety of flexural buckling due to the compressive flange between webs. This FOS value had a value of 0.615, indicating that design zero cannot support the load of the train without further modifications.

2.2 Design #1

We decided that an increase of the thickness of the "top sheet" (area where flexural buckling due to the compressive flange between webs was occuring) was ideal, since the critical stress of this area is dependent on a greater thickness. Doing so, improved resistance to the buckling of compressive flange between webs dramatically, to a number of 3.96. Our lowest factor of safety was 1.667, and came from failure of compression at the top.

2.3 Design #2

In order to increase this factor of safety, we decided to increase our height to 120 mm and decrease our base to 70 mm. The idea behind doing so, was that we increase the location of the centroid ($\bar{y}$) such that the distance from the top of the beam to $\bar{y}$ increases, decreasing the maximum stress at the bottom. We took into consideration that increasing the overall sectional area also increases the second moment of area (I) value, ultimately decreasing our stress at the top (following the $\frac{My}{I}$ equation). Nonetheless, our stress at the top was 2.10 and our factor of safety came out to be 2.86. In addition, diaphragms were added at 150 mm spacings in order to further reinforce the beam: doing so increased our factor of safety of shear buckling 7.14.

2.4 Design #3

In the third design we decided to get more creative with our bridge, as materials became a very tight constraint. The first 250 mm of length of the bridge had a doubled thickness on the top sheet and a base. The height and width of this first section were 130 mm and 60 mm, respectively. This further raised our $\bar{y}$, as desired. The following 200 mm segments on each side had no bases. They still followed the previous dimensions of 130 by 60 and had a double layering on the top sheet. Finally, the middle 400 mm section was triple layered and baseless. It still followed the same dimensions as the previous sections. Overall, the lowest factor of safety for this iteration was 2.89, however maximum materials would have been exceeded as simulated with an online software called CutList Optimizer.

2.5 Design #4

The fourth design involved reconsidering how feasible gluing a thin area was and how feasible our bridge was in respect to the provided materials. We decided to increase the gluing area to 10 mm, as we believed that it was easier to glue on that surface. The height was also brought up to 140 mm, to change the $\bar{y}$ position. All other dimensions were kept the same as for Design #3. After running these numbers through our program we produced a large factor of safety of 3.46. As hopeful as these changes were, they made this design impossible to create, due to the fact that no matter how hard we optimized our dimensions, we could not sketch this on the matboard provided, meaning excess material would be required. This forced us to make several changes, forcing our fifth and final design.

3. Construction Process

3.1 Board optimization

In order to be as efficient as possible with the provided board, careful calculations of each dimension of each segment in our bridge were required. We uploaded the segment dimensions to CutList Optimizer, where an image of the required optimal cuts was given. Tracing before the cuts was done to pre-determine how cutting should be carried out, and to visualize how much of the board is left over for harder to calculate components of our design, such as splice connections.

Figure 1: Tracing on the matboard.

3.2 Cutting and Gluing

After tracing, the desired cuts were performed. This was done using a boxercutter that was dragged across the traced lines. It was important to cut exactly on the line, rather than around them, as all measurement lines were drawn at the exact millimeter of the desired cut.

Figure 2: Cutting out pieces of the bridge.

Gluing was a much more difficult process that involved patience and diligence, to maximize the glue strength. At certain parts of the bridge, the glue was applied and carefully held by team members until 20 minutes passed, in order to ensure that the glue hardened. This method of using a member to hold the piece that is being glued was usually used for smaller pieces such as the diaphragms. At larger points of the bridge, after applying the glue, wooden beams were used to hold the pieces that are being glued together in place, in order for them to dry. The wooden beams were also great for compressing the glue, to have the pieces connect tightly. The fans of the Myhal basement were also used to assist in the drying of the glue, and were useful to save time. Glue was often reapplied to various parts of the bridge in order to ensure maximum strength.

Figure 3: Wooden beams used to hold glued pieces.

Figure 4: Wooden beams used to compress drying pieces.

3.3 Splice Decisions

Deciding where the splices were located on our bridge was a critical component of increasing bridge strength. Two considerations were taken into account when making these splice improvements. The first was that the several layers of the top sheet of the deck must alternate when connecting them in order to minimize the number of matboard additions to be made. The second, was adding horizontal patches between the different bridge components to connect the different segments. These were chosen to be horizontal, as we believe that the second moment of inertia at these patches will be high due their geometry.

Figure 5: Gluing the layers of the top sheet in an alternating pattern.

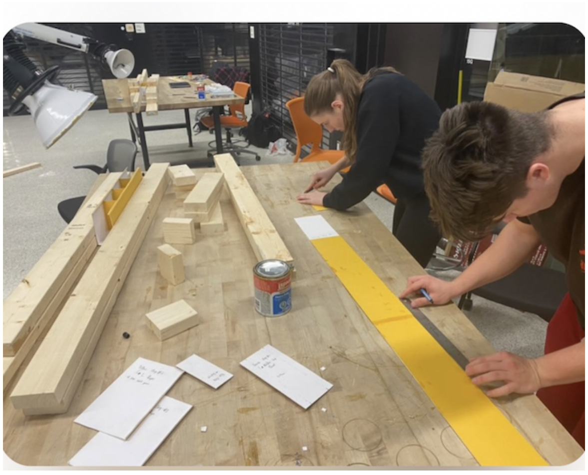

Figure 6: The attached horizontal patches.

3.4 Final Product

Below is an image of our final product, with the bottom facing upwards. This is what we referred to as Design #5.

Figure 7: The final product.

4. Appendix A

Figure 8: Design 0 FOS values, measured in MPa, generated from the MATLAB code

Variable	Value
FOS tension	4.35
FOS compression	1.034
FOS shear ultimate	2.67
FOS shear glue	7.49
FOS buckling 1	0.615
FOS buckling 2	3.58
FOS buckling 3	5.27
FOS shear buckling	3.50

Figure 9: Design 1 FOS values, measured in MPa, generated from the MATLAB code

Variable	Value
FOS tension	4.71
FOS compression	1.662
FOS shear ultimate	2.69
FOS shear glue	6.20
FOS buckling 1	3.96
FOS buckling 2	23.1
FOS buckling 3	14.94
FOS shear buckling	3.78

Figure 10: Design 2 FOS values, measured in MPa, generated from the MATLAB code

Variable	Value
FOS tension	8.48
FOS compression	2.86
FOS shear ultimate	4.21
FOS shear glue	10.45
FOS buckling 1	8.93
FOS buckling 2	18.34
FOS buckling 3	8.41
FOS shear buckling	7.14

Figure 11: Design 3 FOS values, measured in MPa, generated from the MATLAB code

Variable	Value
FOS tension	5.48
FOS compression	2.89
FOS shear ultimate	4.47
FOS shear glue	11.23
FOS buckling 1	12.35
FOS buckling 2	10.63
FOS buckling 3	7.51
FOS shear buckling	10.37

Figure 12: Design 4 FOS values, measured in MPa, generated from the MATLAB code

Variable	Value
FOS tension	6.217
FOS compression	3.46
FOS shear ultimate	4.81
FOS shear glue	23.4
FOS buckling 1	12.56
FOS buckling 2	16.85
FOS buckling 3	8.41
FOS shear buckling	10.89

Figure 13: Design 5 FOS values, measured in MPa, generated from the MATLAB code

Variable	Value
FOS tension	5.48
FOS compression	3.22
FOS shear ultimate	4.15
FOS shear glue	9.79
FOS buckling 1	13.77
FOS buckling 2	5.38
FOS buckling 3	11.91
FOS shear buckling	3.41